



## ARTICLE

# Molecular basis of the interaction of Hsp90 with its co-chaperone Hop

Antonia Lott<sup>1</sup> | Javier Oroz<sup>1</sup>  | Markus Zweckstetter<sup>1,2</sup> 

<sup>1</sup>German Center for Neurodegenerative Diseases (DZNE), Göttingen, Germany

<sup>2</sup>Department for NMR-Based Structural Biology, Max Planck Institute for Biophysical Chemistry, Göttingen, Germany

## Correspondence

Markus Zweckstetter, German Center for Neurodegenerative Diseases (DZNE), Von-Siebold-Str. 3a, 37075 Göttingen, Germany.  
Email: markus.zweckstetter@dzne.de

## Funding information

Deutsche Forschungsgemeinschaft, Grant/Award Number: SFB860; H2020 European Research Council, Grant/Award Number: 787679

## Abstract

The heat shock protein (Hsp) Hsp90 is one of the most abundant proteins in the cell. It controls the functional turnover of proteins being involved in protein folding, refolding, transport as well as protein degradation. Co-chaperones influence Hsp90's activity in different ways, among which the Hsp organizing protein (Hop) was found to inhibit its ATP hydrolysis upon binding. Despite the availability of a number of studies investigating the Hsp90:Hop complex, several aspects of the Hsp90:Hop interaction have remained unresolved. Here, we employed a combinatory approach comprising native polyacrylamide gel electrophoresis, isothermal titration calorimetry, multiangle light scattering, isothermal titration calorimetry, small-angle X-ray scattering, dynamic light scattering, and nuclear magnetic resonance, spectroscopy to obtain a comprehensive picture about the human Hsp90 $\beta$ :Hop association in solution. Our data show that only one Hop molecule binds the Hsp90 $\beta$  dimer, Hop can interact with the open and closed state of Hsp90 $\beta$ , and Hop's TPR2A-2B domains determine the affinity for Hsp90's C-terminal and middle domain, whereby the interaction with the C-terminal domain of Hsp90 $\beta$  is sufficient to induce an allosteric conformational change between the two Hsp90 $\beta$  monomers in the Hsp90<sub>2</sub>:Hop<sub>1</sub> complex. Together, this study highlights the important role of the co-chaperone Hop in reorganizing Hsp90 for efficient client loading.

## KEYWORDS

co-chaperone, Hop, Hsp90, TPR domain

**Abbreviations:** ADP, adenosine diphosphate; Aha1, Activator of 90 kDa heat shock protein ATPase homolog 1; AMP-PNP, adenylyl-imidodiphosphate; ATP, adenosine triphosphate; cl, charged linker; CSP, chemical shift perturbation; DLS, dynamic light scattering; DP, Asp/Pro rich domain; DTT, dithiothreitol; *E. coli*, Escherichia coli; EDTA, ethylenediaminetetraacetic acid; EM, electron microscopy; Hop, Hsp organizing protein; Hsp90, heat shock protein 90; I, intensity; Ile, isoleucine; IPTG, isopropyl- $\beta$ -D-thiogalactopyranoside; ITC, isothermal titration calorimetry;  $K_D$ , dissociation constant; kDa, kilodalton; LB, Luria Broth medium; MALS, multiangle light scattering; MHz, megahertz; MW, molecular weight; Ni-NTA, nickel-nitrilotriacetic acid; NMR, nuclear magnetic resonance; o/n, over night; OD<sub>600</sub>, optical density at  $\lambda = 600$  nm; Page, polyacrylamide gel electrophoresis; PDB, Protein Data Bank; PMSF, phenylmethylsulfonylfluoride; rpm, rounds per minute; SAXS, small-angle X-ray scattering; SEC, size exclusion chromatography; TPR, tetratricopeptide repeats; TROSY, transverse relaxation optimized spectroscopy;  $\beta$ -ME,  $\beta$ -mercaptoethanol.

This is an open access article under the terms of the Creative Commons Attribution-NonCommercial-NoDerivs License, which permits use and distribution in any medium, provided the original work is properly cited, the use is non-commercial and no modifications or adaptations are made.

© 2020 The Authors. *Protein Science* published by Wiley Periodicals LLC on behalf of The Protein Society.

## 1 | INTRODUCTION

The chaperone cycle of the heat shock protein (Hsp) Hsp90 plays an important role in protein folding, refolding, transport as well as protein degradation. Studies with different members of the Hsp90 family revealed a highly dynamic chaperone that binds and hydrolyzes ATP.<sup>1–9</sup> Hsp90s are multidomain chaperones and function as homodimers. Each Hsp90 monomer is composed of three domains consisting of an N-terminal nucleotide binding domain, the middle and the C-terminal domain. The latter is necessary for dimerization and includes a conserved MEEVD sequence necessary for interactions with proteins containing tetratricopeptide repeat (TPR) motifs.<sup>10–12</sup>

The chaperone's ATPase activity is associated with large conformational changes from an apo-extended to a closed, ATP hydrolysis-compatible state.<sup>5,13</sup> In this process, the eukaryotic Hsp90 interacts with a series of co-chaperones that regulate the structural rearrangements and stabilize nucleotide-state specific conformations.<sup>13–17</sup> As such, the co-chaperone Hop (Hsp-organizing protein) was found to bind in the early stages of the chaperone cycle arresting Hsp90 in an ATP hydrolysis inactive state.<sup>18–20</sup> The Hop multidomain protein consists of three distinct TPR domains (each one comprising three TPR repeats) and two aspartate-proline rich segments (DP) arranged as TPR1-DP1-TPR2A-TPR2B-DP2.<sup>21</sup> The chaperone:Hop association occurs via the TPR domains, whereby TPR2A represents the main interaction site for Hsp90 binding to the C-terminal MEEVD sequence.<sup>22</sup> Hop's DP domains and especially DP2 are important for client activation *in vivo*.

Despite the importance of the Hsp90:Hop interaction for the activity of Hsp90 in eukaryotic cells, the structural properties of the Hsp90:Hop association have not yet been fully resolved.<sup>21,23–26</sup> The major challenge in the structural analysis of the Hsp90:Hop complex lies in the dynamic character and intrinsic flexibility of both Hsp90 and Hop limiting the resolution of electron microscopy (EM) data. This scarce structural data raised divergent models including ambiguous Hsp90 conformations and complex stoichiometries.<sup>23,24</sup>

Hence, the key aim of this study was to gain further insight into the conformation and structural architecture of the Hop-bound Hsp90 in solution. We used wild-type and full-length human proteins to take into account the full complexity of the interaction. Isothermal titration calorimetry (ITC) in combination with multiangle light scattering identified a complex formed by dimeric and monomeric Hsp90 $\beta$  and Hop, respectively. Native polyacrylamide gel electrophoresis (PAGE), small-angle X-ray scattering (SAXS), size exclusion chromatography (SEC),

and dynamic light scattering (DLS) further demonstrated that Hop associates with both the open and closed state of Hsp90 $\beta$ , neither driving an open-closed nor a closed-open change. In addition, data from nuclear magnetic resonance (NMR) spectroscopy show that Hop's TPR2A-2B domains determine its affinity for a broad interaction site within Hsp90's C-terminal and middle domain, and are best in agreement with a mechanism in which the interaction of one Hop molecule induces an allosteric conformational change between the two Hsp90 $\beta$  molecules that stabilizes the chaperone in a V-shaped conformation.

## 2 | RESULTS

### 2.1 | Hop binds Hsp90 with high affinity

The interaction between human Hsp90 $\beta$  (further termed Hsp90) and Hop was analyzed by native page. With increasing amounts of Hop the intensity of the free Hsp90 band decreased while simultaneously an additional band emerged, which increased with increasing Hop concentration, indicative for Hsp90:Hop complex formation (Figure S1a). At the same time, a set of other bands appeared, but these did not become more intense with increasing Hop concentration and were therefore not further considered.

Because Hsp90 consumes ATP, we further tested whether the presence of a nucleotide affects the Hsp90:Hop association. Hop is reported to be present in the initial states of the hydrolysis cycle impairing the ATPase activity of Hsp90 upon binding.<sup>18–20</sup> Hence, we used the non-hydrolysable ATP-analogue adenylyl-imidodiphosphate (AMP-PNP) to convert and retain Hsp90 in its ATP bound state. Quantification of the single Hsp90 band revealed that the Hsp90:Hop interaction is occurring in both the absence and the presence of AMP-PNP (Figure S1b). Further analysis by SEC showed that Hop can interact with both the open and closed conformation of Hsp90 (Figure S1c,d). We observed a preference for the open Hsp90 state, as less free Hop eluted from the column in the absence of AMP-PNP shown in the chromatogram and by SDS-page analysis of the elution fractions. In addition, we collected data from DLS to determine the respective hydrodynamic radii  $R_h$  (Figure S1e). The addition of Hop resulted in an increase of the  $R_h$  of the open Hsp90 indicating complex formation. For the closed Hsp90 we however detected a decrease of the  $R_h$  in the presence of Hop. We ascribe this observation to a distinct amount of free Hop in solution due to the decreased interaction of Hop with the closed state of Hsp90. The combined analysis shows that Hop neither induces an open-close nor a close-open change of Hsp90.

Based on Hop's preference for the open Hsp90 conformation, we performed the subsequent experiments in the absence of AMP-PNP. ITC showed that Hop binds to Hsp90 with high affinity yielding a dissociation constant of  $K_D = 0.6 \mu\text{M}$ , which is in agreement with previous data (Figure 1a).<sup>23</sup> Thermodynamic characterization revealed that the binding of Hop to Hsp90 induces conformational changes and involves the formation of hydrogen bonds as indicated by the unfavorable entropy ( $-\text{T}\Delta\text{S}$ ) and the

favorable binding enthalpy ( $\Delta\text{H}$ ), respectively (Figure 1b). The corresponding stoichiometry of  $N = 0.5$  revealed that only one out of two possible binding sites on Hsp90 is occupied, indicating complex formation in a ratio of 1:2 where one Hop molecule binds to an Hsp90 dimer. Our results are consistent with recent SEC–multiangle light scattering (MALS) experiments that indicate a stable 1:2 association,<sup>24</sup> but contrary to earlier ITC data that conclude an Hsp90:Hop complex in a ratio of 1:1.<sup>23</sup>

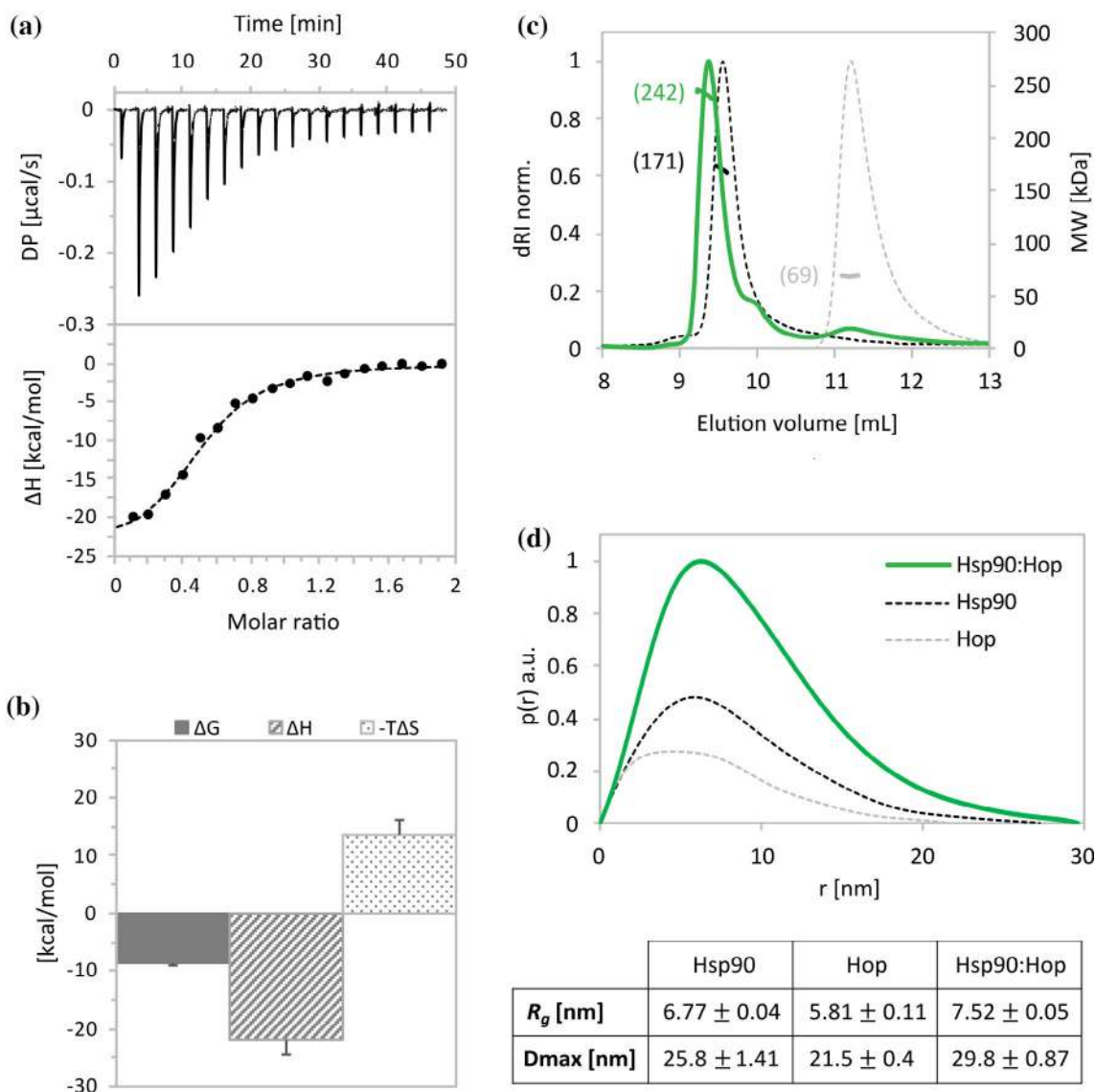


**FIGURE 1** One Hop molecule holds the Hsp90 dimer in a largely extended conformation. (a) Isothermal titration calorimetry (ITC) affinity measurement fitted to a single binding site model ( $K_D = 0.578 \pm 0.073 \mu\text{M}$ ). The stoichiometry of  $n = 0.544 \pm 0.052$  indicates an Hsp90 dimer bound by only one Hop molecule. (b) The interaction of Hsp90 and Hop is characterized by negative  $\Delta\text{H}$  and positive  $-\text{T}\Delta\text{S}$ . Errors represent the  $SD$  out of three independent experiments. (c) Molecular weight determination of the Hsp90:Hop complex by size exclusion chromatography–multiangle light scattering (SEC–MALS) confirms formation of a Hsp90<sub>2</sub>:Hop<sub>1</sub> complex ( $242.2 \pm 2.53$  kDa, green line). Reference elution chromatograms of Hsp90 ( $170.7 \pm 1.99$  kDa, black dotted line) and Hop ( $69.3 \pm 0.29$  kDa, gray dotted line) are shown for comparison. (d) Pair distance distribution functions from SEC–SAXS analysis of Hsp90, Hop, and the Hsp90:Hop complex (same color code as in (c))

## 2.2 | Extended conformation of the 240 kDa Hsp90<sub>2</sub>:Hop<sub>1</sub> complex

To test if the Hsp90:Hop complex is stable during SEC, we performed SEC-MALS experiments for Hop, Hsp90 and the preassembled full-length Hsp90:Hop complex (Figure 1c).<sup>24</sup> In our experimental conditions, the determined mass of 69 kDa and 171 kDa refers to a monomeric Hop (65 kDa) and a dimeric Hsp90 (171 kDa) for the individual proteins, respectively. When incubating both proteins together prior to the SEC-MALS run, we observed a peak shift to earlier elution volume confirming complex formation associated with a higher mass. The calculated molecular weight of 242 kDa confirmed a stable Hsp90<sub>2</sub>:Hop<sub>1</sub> protein complex (236 kDa), in agreement with previous observations.<sup>20,24</sup>

Having assured the stability of the complex, we performed SEC-SAXS experiments to gain insights into the structural dimensions of the Hsp90:Hop complex in solution. The radii of gyration ( $R_g$ ) and maximum dimension ( $D_{max}$ ) were calculated from the pair distance distribution functions (Figure 1d). When compared to Hsp90 alone, which is extended in solution,<sup>27</sup> the radius and maximum dimension further increased to  $R_g = 7.52 \pm 0.05$  nm and  $D_{max} = 29.80 \pm 0.87$  nm upon complex formation. The data suggest that the binding of one Hop molecule is sufficient to hold Hsp90 in an extended conformation and confirm that Hop binding does not induce a transition of Hsp90 from the open to the closed state.

## 2.3 | NMR spectroscopy of the 240 kDa Hsp90:Hop complex

To gain further insights into the structural rearrangements within the Hsp90:Hop complex, we collected NMR data of Hsp90 alone and with increasing concentrations of Hop. We chose NMR spectroscopy, because NMR allows the analysis of large and dynamic molecules in solution with residue-specific sensitivity.<sup>28</sup>

We acquired 2D <sup>13</sup>C-<sup>1</sup>H methyl-TROSY spectra of Hsp90 with exclusively [<sup>1</sup>H, <sup>13</sup>C]-labeled Ile- $\delta$ (1)-methyl groups—an approach that has already been successfully used in previous NMR studies with Hsp90.<sup>15,27,29,30</sup> For Hsp90 alone one peak per isoleucine  $\delta$ -methyl group was observed (Figure 2a). Upon stepwise addition of Hop, the signals started to broaden and to shift as quantified in the respective intensity ( $I/I_0$ ) and chemical shift perturbation (CSP) analysis, indicating that the interaction occurs in the slow exchange regime (Figure 2b). At low concentrations of Hop, changes were mainly observed in residues belonging to the C-terminal domain of Hsp90 including Ile485, Ile590, Ile604, and Ile679. This is in agreement

with previous findings that Hop can interact via its TPR2A domain with the C-terminal MEEVD motif of Hsp90.<sup>21</sup> At a molar ratio of 1:0.5 for Hsp90:Hop, however, peak splitting occurred for residues within the N- and middle domains of Hsp90 including the methyl groups of Ile20, Ile75, Ile287, Ile334, Ile376 and Ile407 (marked by black arrows in Figure 2a). Signal splitting refers to another set of NMR peaks that appear at the cost of the intensity of the original peaks. This peak splitting observed for individual isoleucine  $\delta$ -methyl moieties corresponds to two populations of Hsp90, being in its unbound and bound state, respectively. At the endpoint of the titration the equilibrium was pushed toward the Hop-bound state of Hsp90 as evidenced by the decrease of the signal intensities from the free Hsp90 down to on average 30% (Figure 2b), while the signals from Hsp90 as part of the Hsp90:Hop complex were increased. Notably, as we passed a 50:50 distribution of the signal intensities from unbound and bound state, we conclude that both Hsp90 arms undergo a conformational change. In combination with the results from ITC and SEC-MALS (Figure 1), which showed that only one Hop molecule binds the Hsp90 dimer, the NMR analysis provides support for an allosteric communication between the two Hsp90 monomers.

We mapped the Hop-perturbed residues at the 1:1 titration point onto the available, closed structure of human Hsp90 (Figure S2).<sup>8</sup> The interaction with Hop affected Hsp90 residues within every domain of the chaperone. If the closed state was the Hop-induced conformation of Hsp90, we would expect perturbations of residues within the dimer interface, as previously observed for the Hsp90:Aha1 complex.<sup>30</sup> However, within the Hsp90:Hop complex the Hsp90 dimer interface remained unperturbed. The binding of Hop thus does not induce the closed conformation of Hsp90, in agreement with the extended shape observed by SEC-SAXS (Figure 1d).

Next, we mapped the Hop-induced perturbations onto a previously generated open model of the Hsp90 dimer structure (Figure 2c).<sup>27</sup> The perturbed isoleucine methyl groups define two regions, one in the C-terminal domain and a second region in the middle domain, which face each other (marked with two black lines in Figure 2c). This observation suggests two possible scenarios: (a) Hop binds to these regions, thereby blocking the closure and stabilizing Hsp90 in an open conformation, or alternatively (b) Hop binds to Hsp90-C evoking the rearrangement of Hsp90 toward a V-shaped conformation as illustrated in Figure 2c. A V-shaped Hop-stabilized conformation of Hsp90 has recently been suggested by low-resolution cryo-EM.<sup>24</sup> In this V-shaped model of the Hsp90:Hop complex, the N-terminal domains of Hsp90 are rotated by 90° toward the ATP-

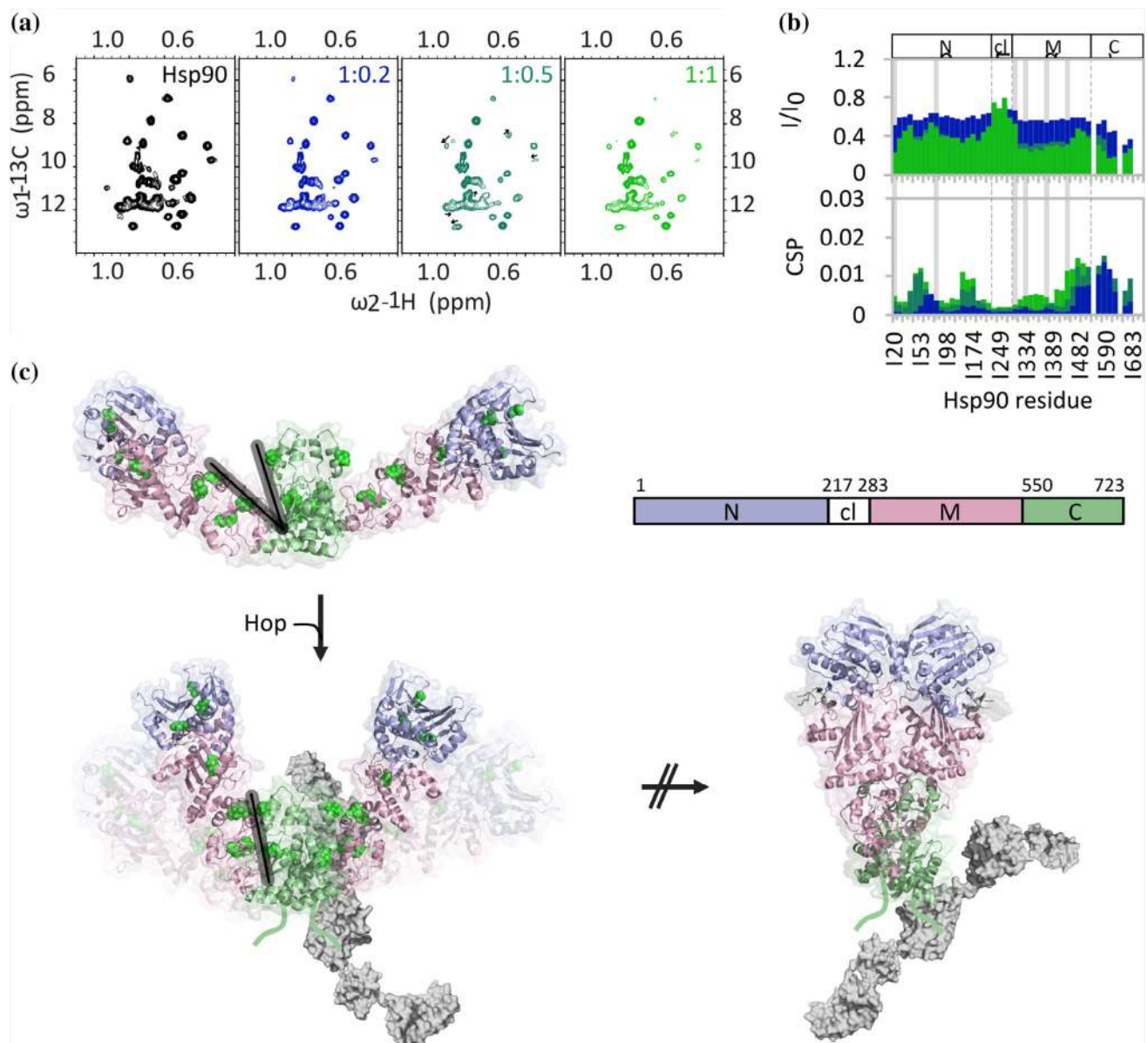


**FIGURE 2** Nuclear magnetic resonance (NMR) spectroscopy of the 240 kDa Hsp90:Hop complex. (a) 2D  $^{13}\text{C}$ - $^1\text{H}$  methyl-TROSY spectra of Hsp90 alone (black) and in the presence of increasing concentrations of Hop (1:0.2 blue, 1:0.5 turquoise, 1:1 green; black arrows mark the observed peak splitting between the free and the bound state of Hsp90). (b) Peak intensity ( $I/I_0$ ) and chemical shift perturbation (CSP) plots of Hsp90's isoleucine  $\delta$ -methyl groups observed in ((a); same color code). Gray lines highlight residues where peak splitting was observed. Hsp90 domains are depicted on top and represented with dotted lines within each graph. (c) Domain organization of Hsp90 (N—N-terminal domain, purple; cl—charged linker, white; M—middle domain, pink; C—C-terminal domain, green). Front view of the open conformation of Hsp90 depicted as cartoon. Hop affected isoleucine residues are highlighted in light green and represented as spheres. Perturbations observed in the NMR spectra in (a) can be ascribed to a conformational rearrangement of Hsp90 into a V-shape when bound by Hop (left). The corresponding interface between Hsp90's C-terminal and middle domain is marked with black lines. Hop, depicted with a gray surface, interacts via its TPR2A domain with Hsp90's C-terminal MEEVD motif<sup>22</sup> represented as green line—the only accessible interaction site when Hsp90 is closed (right). The crossed-out arrow illustrates that Hop binding does not induce an open-close change

bound state. This in turn could indicate that the Hop-induced signal perturbations, which we observed within the N-terminal of Hsp90 (Figure 2b,c), are caused by conformational changes induced by Hop but not due to a direct interaction of Hop with the N-terminal domain of

Hsp90. We also note that the perturbed residues within the C-M interface are not accessible when Hsp90 is in its closed conformation (Figure S2). This could indicate a smaller interaction interface for Hop with Hsp90 closed (Figure 2c)—the structural basis for Hop's preference for

the open conformation of Hsp90 observed by SEC and DLS (Figure S1c–e).

## 2.4 | Stabilization of Hsp90 in largely extended conformation

In order to provide additional support for the Hop-induced stabilization of Hsp90 in a largely extended, possibly V-shaped conformation, we prepared a shorter Hop construct comprising only the first three domains including TPR1, DP1, and TPR2A (termed Hop112a; Figure 3a).

Hop112a is sterically unable to reach Hsp90-N when bound to the MEEVD motif within Hsp90-C.<sup>21</sup> Hence, if we detect the same perturbations in the presence of Hop112a as with full-length Hop the interaction with Hsp90-C is sufficient to stabilize Hsp90 in a V-shaped conformation with the N-terminal domains rotated toward the nucleotide bound state as described previously.<sup>24</sup>

To this end, we first investigated the Hsp90:Hop112a interaction via native page as described above for full-length Hop (Figure S3a). The appearance of an Hsp90:Hop112a complex band demonstrated complex formation. We then compared the intensity decrease of the free Hsp90 band for

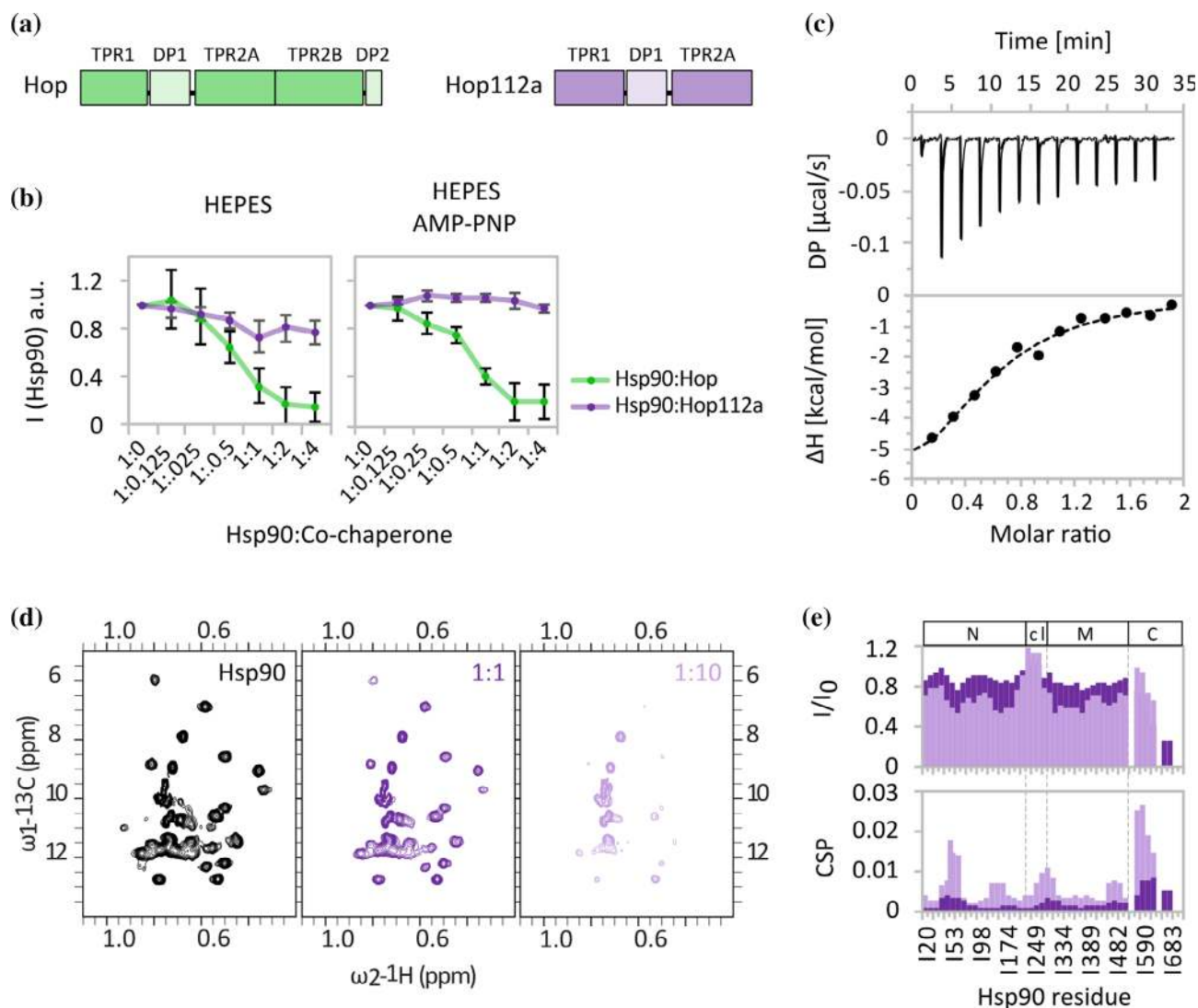


**FIGURE 3** Interaction of the truncated Hop construct Hop112a with Hsp90. (a) Domain organization of Hop and Hop112a. (b) Quantitative analysis of the native page in Figures S1 and S3 displaying the amounts of free Hsp90 at increasing concentrations of Hop112a (purple) or full-length Hop (green) in the absence (left) and the presence (right) of adenylyl-imidodiphosphate (AMP-PNP). (c) Isothermal titration calorimetry (ITC) affinity measurement (top) fitted to a single binding site model (bottom) of Hop112a-binding to Hsp90. (d) 2D <sup>13</sup>C-<sup>1</sup>H methyl-TROSY spectra of Hsp90 alone (black) and in the presence of increasing concentrations of Hop112a (1:1 dark purple, 1:10 light purple). (e) Peak intensity (I/I<sub>0</sub>) and chemical shift perturbation (CSP) plots of Hsp90's isoleucine δ-methyl groups observed in ((d); same color code). Hsp90 domains are depicted on top and represented with dotted lines within each graph

increasing amounts of Hop and Hop112a, respectively. The comparison showed that with the shorter Hop112a construct higher ratios are necessary to reach equivalent amounts of Hsp90:co-chaperone complex (Figure 3b, left). The preference of Hop to bind the apo over the AMP-PNP-bound Hsp90 also became slightly more pronounced (Figure 3b, right). The observations from native page were further supported with affinity measurements by ITC revealing an approximately 10-times lower affinity of Hop112a for Hsp90 ( $K_D = 3.59 \pm 1.07 \mu\text{M}$ ) when compared to full-length Hop (Figure 3c). The decreased binding affinity after the removal of the TPR2B-DP2 domains is in agreement with previous experiments studying the interaction of different Hop domains with Hsp90 peptides.<sup>21,31</sup> In these studies, it was concluded that the rigid structure between the TPR2A and TPR2B domain accounts for a stable Hop-TPR2A:Hsp90-C association.<sup>21</sup> However, the stoichiometry of  $N = 0.50 \pm 0.09$  indicates that the binding behavior is identical to full-length Hop, and one Hop112a molecule binds to an Hsp90 dimer.

We then collected 2D  $^{13}\text{C}$ - $^1\text{H}$  methyl-TROSY spectra of Hsp90 with increasing amounts of Hop112a (Figure 3d). Consistent with its diminished Hsp90-binding affinity, 10-times higher amounts of Hop112a were necessary to observe a similar extent of signal changes in the Hsp90 spectra. Quantitative analysis of the signal intensities and CSPs were similar to those observed in Hsp90 upon binding to full-length Hop (Figures 3e and S3b). Signal perturbations were detected for the same residues located in the V-interface and in Hsp90-N (Figure S3b).<sup>24,25</sup> However, due to its smaller size, Hop112a affected a slightly smaller region within the C-M interface compared to full-length Hop, potentially contributing to its lower Hsp90 affinity (Figures 2c and S3). Altogether, we conclude that the interaction between Hop(112a) and the C-terminal domain of Hsp90 is sufficient to induce conformational changes in Hsp90-N and stabilize Hsp90 in a V-shaped conformation in the Hsp90:Hop complex.

### 3 | DISCUSSION

Hop is one of the best characterized TPR-domain containing co-chaperones of Hsp90. However, this brought along diverse and sometimes discrepant conceptions regarding the composition of the Hsp90:Hop complex. Our biochemical characterization of the interaction between full-length human Hsp90 $\beta$  and Hop demonstrated a stoichiometry of 2:1, where one Hop molecule binds the dimeric Hsp90. These observations are in contrast to previous studies from Onuoha et al. who described a dimeric Hop protein,<sup>23</sup> though overlaps with more recent data where Hop was found to be

monomeric.<sup>20,24,32</sup> In addition, we observed NMR peak splitting at an Hsp90:Hop molar ratio of 1:0.5 affirming a stable interaction at half amount of Hop compared to Hsp90. Hence, our data endorse the latest assumption of a stable Hsp90:Hop complex in a ratio of 2:1.<sup>24–26</sup>

The combination of SEC-SAXS and NMR experiments showed that Hsp90 $\beta$  remains in a largely extended, V-shaped conformation. The largely extended conformation of Hsp90 in complex with Hop is inconsistent with a model of the Hsp90:Hop complex suggested on the basis of negative stain EM where the chaperone is embedded into the Hsp90:Hop density in its semiclosed, ADP-bound state.<sup>13,26</sup> Our data, however, agree with a low-resolution structural characterization of the Hsp90 $\alpha$ :Hop complex by cryo-EM.<sup>24,25</sup> Indeed, the NMR-observed perturbations are consistent with a V-shaped interface between the middle and the C-terminal domain of Hsp90 $\beta$  (Figure 2c). Moreover, our data provide experimental support for an allosteric communication between the two Hsp90 $\beta$  monomers, as the binding of only one Hop molecule induces a conformational change in both arms of the Hsp90 $\beta$  dimer. The consistent result for different Hsp90 variants (Hsp90 $\beta$  this work and Hsp90 $\alpha$  in Reference 24) indicates that the Hsp90:Hop interaction is similar for the constitutively expressed and the stress-inducible Hsp90. Notably, to generate a more stable Hsp90 $\alpha$ :Hop complex applicable to cryo-EM, disulfide bonds between Hsp90 $\alpha$  and Hop had been used, which might result in non-native interactions. Indeed, the cryo-EM model includes two Hop proteins—a possibility that we ruled out as described above. Nevertheless, the combined data from cryo-EM and NMR provide strong support for the formation of a V-shaped conformation of the Hsp90:Hop complex.

We also detected NMR signal perturbations of residues within the N-terminal domain of Hsp90 $\beta$  (Figure 2), in agreement with results from the Agard group who observed a Hop-induced 90° rotation of the N-terminal domain of Hsp90 $\beta$  by cryo-EM.<sup>24</sup> However, with the use of full-length Hop we were not able to affirm whether the changes in the N-terminal domain of Hsp90 $\beta$  arise from a direct interaction with Hop, or are a result of conformational changes induced by Hop binding to Hsp90-C. For that reason, we made use of a shorter Hop construct named Hop112a being unable to reach Hsp90-N when bound to the C-terminal domain of Hsp90 $\beta$ .<sup>21</sup> As we further detected the same signal attenuations in Hsp90-N as with full-length Hop, we conclude that the binding to Hsp90-C is sufficient to induce the conformational changes in Hsp90-N. Hence, our data affirm an Hsp90 $_2$ :Hop $_1$  complex with Hsp90's N-terminal domains rotated inward.

Notably, the 90° rotation implicated in the cryo-EM model of the Hsp90 $\alpha$ :Hop complex displays Hsp90-N in its ATP-bound conformation.<sup>24</sup> In our Hsp90 $\beta$ :Hop interaction studies by native page, we did not observe a decisive tendency toward the nucleotide-free or -bound state. This indicates that Hop binds Hsp90 $\beta$  independent of whether the chaperone is present in its apo or ATP-bound state. However, once Hop is bound, the N-terminal domain of Hsp90 $\beta$  is stabilized in its ATP-conformation. Consistent with this hypothesis, the  $k_{\text{off}}$  and  $k_{\text{on}}$  rates of ATP binding are increased in the presence of Hop, although the Hsp90's ATP-affinity is overall unchanged.<sup>19</sup>

We observed that Hop interacts with both the open and the closed conformation of Hsp90 $\beta$ , but has a preference for the open state. In agreement with this preference for the open state of Hsp90 $\beta$ , NMR spectroscopy showed that an additional Hop-interaction site is present when Hsp90 is in the open conformation, while this binding site is not accessible when Hsp90 is closed. With regard to Hsp90's ATP hydrolysis cycle, Hop was so far known to be released upon Hsp90 closure.<sup>13</sup> Our findings showing Hop binding to the closed state of Hsp90 however suggest that Hsp90:substrate or Hsp90:substrate:co-chaperone complexes, in which Hsp90 is present in the closed conformation, additionally can exhibit Hop bound to Hsp90. Notably, Hop binding did not evoke the transition of Hsp90 from the open to its closed conformation or vice versa, indicating that Hop bound to such higher order complexes has no active but possesses merely a stabilizing function.

Although the major Hsp90:Hop interaction occurs via the TPR2A domain of Hop binding to the MEEVD motif located in the C-terminal domain of Hsp90,<sup>21,22</sup> we observed an approximately 10-times decreased binding affinity of the shorter Hop112a construct for Hsp90 $\beta$  compared to full-length Hop (Figure 3). Previous studies with different modules of the Hop protein revealed that the combined TPR2A-TPR2B segment is essential to observe significant inhibition of the ATPase activity of Hsp90.<sup>21</sup> It was further shown that only in the presence of the rigid linker, not only connecting the two TPR domains but holding them in a fixed orientation, the inhibitory function of Hop is sustained *in vivo*.<sup>21</sup> Hence, in combination with the results presented here we conclude that upon removal of the TPR2B domain associated with the rupture of the linker region, the interaction with Hsp90 is diminished and the Hop-based inhibition of the Hsp90's ATP hydrolysis is impaired.

In conclusion, our findings depict a comprehensive picture of the human Hsp90 $\beta$ :Hop interaction highlighting Hop as an essential regulator of Hsp90 action.

## 4 | MATERIALS AND METHODS

### 4.1 | Protein expression and purification

Human Hsp90 $\beta$  (HSP90AB1) was expressed in *Escherichia coli* Rosetta2 (DE3) strain growing in LB medium for 4 hr at 37°C with 110 rpm stirring speed. Protein over-expression was induced at OD<sub>600</sub> = 0.8 with 1 mM IPTG. Cells were harvested and lysed by sonication in 20 mM Tris pH 8.0/500 mM NaCl/10 mM Imidazole/6 mM  $\beta$ -ME/1  $\mu$ M PMSF/1 tablet of protease inhibitor. The supernatant including His<sub>6</sub>-tagged Hsp90 was further purified by Ni-NTA affinity chromatography with gravity flow and eluted in 20 mM Tris pH 8.0/300 mM NaCl/250 mM Imidazole/6 mM  $\beta$ -ME. Residual impurities were removed by SEC using an SD200 26/600 column (using 2 ml/min flow) preequilibrated in 10 mM HEPES pH 7.5/500 mM KCl/0.5 mM DTT. Fractions of interest were dialyzed *o/n* into 25 mM HEPES pH 7.4/100 mM KCl/5 mM MgCl<sub>2</sub>/1 mM TCEP and used for further experiments.

For NMR experiments, human Hsp90 $\beta$  was produced in *E. coli* BL21 (DE3) as [<sup>15</sup>N, <sup>13</sup>C, <sup>2</sup>H] protein with selectively labeled [<sup>1</sup>H-<sup>13</sup>C]-isoleucine  $\delta$ (1)-methyl groups as described previously.<sup>9</sup> Protein purification was carried out as described above and dialyzed in 25 mM HEPES pH 7.4/100 mM KCl/5 mM MgCl<sub>2</sub>/1 mM TCEP (99% D<sub>2</sub>O) for subsequent NMR experiments.

Full-length human Hop (STIP1) as well as the shorter Hop112a construct (aa. 1–352) were expressed *o/n* in *E. coli* Rosetta2 (DE3) growing in LB medium at 20°C induced at OD<sub>600</sub> = 0.6 with 0.1 mM IPTG. Cells were harvested and lysed by sonication in 20 mM Tris pH 8.0/500 mM NaCl/10 mM Imidazole/3 mM  $\beta$ -ME/1  $\mu$ M PMSF/1 tablet of protease inhibitor. His<sub>6</sub>-tagged Hop and Hop112a was further purified by Ni-NTA affinity chromatography with gravity flow and eluted in 20 mM Tris pH 8.0/500 mM NaCl/500 mM Imidazole/3 mM  $\beta$ -ME. For the Hop112a protein, the tag was cleaved off with thrombin protease in 25 mM Tris pH 8.0/100 mM NaCl/3 mM  $\beta$ -ME followed by a second Ni-NTA affinity chromatography to remove potential uncleaved fractions. For both Hop and Hop112a, residual impurities were removed by SEC using an SD75 26/600 (2 ml/min) preequilibrated in 25 mM HEPES pH 7.4/100 mM KCl/5 mM MgCl<sub>2</sub>/1 mM TCEP (Hop) or 25 mM HEPES pH 7.4/150 mM NaCl/1 mM DTT (Hop112a). Peak fractions were pooled and stored in 25 mM HEPES pH 7.4/100 mM KCl/5 mM MgCl<sub>2</sub>/1 mM TCEP.



## 4.2 | Complex assembly and native page analysis

Protein–protein interactions were enabled during 45 min at 25°C gently shaking at 350 rpm in 25 mM HEPES pH 7.4/100 mM KCl/5 mM MgCl<sub>2</sub>/1 mM TCEP—both in the absence and the presence of 5 mM AMP-PNP. A fixed concentration of 1.25 μM Hsp90 was mixed with increasing concentrations of Hop or Hop112a up to a Hsp90: Hop(112a) molar ratio of 1:4. Complex formation was monitored via native Page using 7.5% precast gels (Mini-Protean TGX; BioRad). The gels were run for 2.5 hr at 110 V. Band intensities were quantified with ImageJ. Errors represent the *SD* out of three independent experiments.

## 4.3 | Molecular weight determination by SEC-MALS

The Hsp90:Hop complex was further analyzed by SEC using a silica-based WTC-050S5 analytical column in line with a DAWN HELEOS II MALS and Optilab T-rEX dRI detector (Wyatt Technology) (0.5 ml/min). As native page showed that maximum complex formation along with minimal excess of residual free proteins was achieved when mixing the proteins in an equimolar ratio, 10 μM of each Hsp90 and Hop were incubated in 25 mM HEPES pH 7.4/10 mM KCl/5 mM MgCl<sub>2</sub> prior to the SEC-MALS run. The SEC-MALS run was performed in the same buffer including 0.02% NaN<sub>3</sub> to avoid bacterial growth. Molecular weights were determined with the ASTRA software package (Wyatt Technology). Errors represent the *SD* of the molecular weights calculated within the selected peak areas.

## 4.4 | Small-angle X-ray scattering

SEC-SAXS experiments were carried out at the Diamond Light Source (UK). Prior to the SAXS measurement, proteins (100 μM Hsp90, 200 μM Hop, 100 μM Hsp90:Hop 1:1) were separated using a Shodex KW403-4F column preequilibrated in 25 mM HEPES pH 7.4/100 mM KCl/5 mM MgCl<sub>2</sub>/1 mM TCEP (0.16 ml/min). Data were processed with ATSAS 2.8.3. Errors represent the *SD* out of three independent experiments.

## 4.5 | Affinity measurements

The affinities of Hop and Hop112a for Hsp90 were analyzed by ITC in 25 mM HEPES pH 7.4/100 mM

KCl/5 mM MgCl<sub>2</sub>/1 mM TCEP. Binding experiments were performed at 25°C on a Microcal PEAQ-ITC automated machine (Malvern). A total volume of 38 μl of Hop or 39 μl of Hop112a (80 μM) was injected into a cell containing 370 μl of Hsp90 (8 μM) (19 injections à 2 μl or 13 injections à 3 μl). Data were analyzed with the instruments control software (MicroCal). Errors represent the *SD* out of three independent experiments.

## 4.6 | DLS and SEC

Hop association with Hsp90 was further analyzed by DLS (DynaPro NanoStar; Wyatt) and SEC using an SD200 10/300 column (0.5 ml/min). Hsp90 and Hop were mixed in an equimolar ratio in 25 mM HEPES pH 7.4/100 mM KCl/5 mM MgCl<sub>2</sub>/1 mM TCEP before analysis (5 μM each). Hsp90 was fixed in its closed conformation by incubating the chaperone for 1.5 hr at 40°C in 25 mM HEPES pH 7.4/100 mM KCl/5 mM MgCl<sub>2</sub>/1 mM TCEP/5 mM AMP-PNP/1 M (NH<sub>4</sub>)<sub>2</sub>SO<sub>4</sub>. Hsp90 closure was verified by a shift to later elution volumes as well as smaller hydrodynamic radii referring to the more compact state. DLS data were analyzed with DYNAMICS (Wyatt Package). SEC elution fractions were analyzed by SDS-page using 7.5% precast gels (Mini-Protean TGX; BioRad).

## 4.7 | 2D <sup>1</sup>H-<sup>13</sup>C methyl-TROSY NMR

Two-dimensional <sup>1</sup>H-<sup>13</sup>C methyl-TROSY NMR spectra were recorded at 25°C on a Bruker Avance 900 MHz spectrometer equipped with a TCI cryogenic probe. NMR data were acquired in 25 mM HEPES pH 7.4/100 mM KCl/5 mM MgCl<sub>2</sub>/1 mM TCEP (99% D<sub>2</sub>O). Total of 50 μM of fully deuterated Hsp90 with exclusively labeled [<sup>1</sup>H-<sup>13</sup>C]-isoleucine δ-methyl groups were measured in the absence and the presence of Hop (1:0.2, 1:0.5, 1:1) and Hop112a (1:1, 1:10). Data were processed in TopSpin (Bruker) and analyzed with Sparky (NMRFAM-SPARKY 1.4). Peak assignments for Hsp90 isoleucine methyl groups were adapted from the literature.<sup>27</sup> Side chain specific CSPs and signal intensities were calculated according to  $CSP = \sqrt{\left(\Delta H^2 + \frac{\Delta C^2}{7}\right)} * \frac{1}{2}$  and  $\frac{I}{I_0}$ , respectively, where  $\Delta H$  is the change in proton chemical shift (ppm),  $\Delta C$  is the change in carbon chemical shift (ppm),  $I$  is the peak intensity of the titration point of Hsp90 with Hop or Hop112a, and  $I_0$  is the peak intensity of the Hsp90 reference spectrum.<sup>33</sup> Structures were displayed via PyMOL (Schrodinger, LLC, 1.8.7.0.). We used the structure of the human Hsp90 deposited in the PDB (PDB code: 5fwk).<sup>8</sup> Residues above the CSP threshold at a 1:1 and 1:10

titration point for Hsp90:Hop and Hsp90:Hop112a, respectively, were mapped onto the Hsp90 structures. The CSP threshold was determined as the *SD* times 1.5.

## ACKNOWLEDGMENTS

The authors thank G. Butnariu for help with the purification of the Hop112a construct. M. Z. was supported by the German Science Foundation through the Collaborative Research Center 860 (project B2), and by the advanced grant “787679 - LLPS-NMR” of the European Research Council. Open access funding enabled and organized by Projekt DEAL.

## CONFLICT OF INTEREST

The authors declare no conflict of interests.

## AUTHOR CONTRIBUTIONS


**Antonia Lott:** Prepared proteins and performed experiments and data analysis. **Javier Oroz:** Performed Hsp90 NMR assignments. **Antonia Lott** and **Markus Zweckstetter:** Designed the project and wrote the paper.

## DATA AVAILABILITY STATEMENT

All data that support the findings of this study are available from the corresponding authors upon reasonable request.

## ORCID

Javier Oroz  <https://orcid.org/0000-0003-2687-3013>

Markus Zweckstetter  <https://orcid.org/0000-0002-2536-6581>

## REFERENCES

- Panaretou B, Prodromou C, Roe SM, et al. ATP binding and hydrolysis are essential to the function of the Hsp90 molecular chaperone in vivo. *EMBO J*. 1998;17:4829–4836.
- Prodromou C, Panaretou B, Chohan S, et al. The ATPase cycle of Hsp90 drives a molecular ‘clamp’ via transient dimerization of the N-terminal domains. *EMBO J*. 2000;19:4383–4392.
- Pearl LH, Prodromou C. Structure and in vivo function of Hsp90. *Curr Opin Struct Biol*. 2000;10:46–51.
- Wandinger SK, Richter K, Buchner J. The Hsp90 chaperone machinery. *J Biol Chem*. 2008;283:18473–18477.
- Richter K, Soroka J, Skalniak L, et al. Conserved conformational changes in the ATPase cycle of human Hsp90. *J Biol Chem*. 2008;283:17757–17765.
- Krukenberg KA, Forster F, Rice LM, Sali A, Agard DA. Multiple conformations of *E. coli* Hsp90 in solution: Insights into the conformational dynamics of Hsp90. *Structure*. 2008;16:755–765.
- Taipale M, Jarosz DF, Lindquist S. HSP90 at the hub of protein homeostasis: Emerging mechanistic insights. *Nat Rev Mol Cell Biol*. 2010;11:515–528.
- Verba KA, Wang RY, Arakawa A, et al. Atomic structure of Hsp90-Cdc37-Cdk4 reveals that Hsp90 traps and stabilizes an unfolded kinase. *Science*. 2016;352:1542–1547.
- Oroz J, Kim JH, Chang BJ, Zweckstetter M. Mechanistic basis for the recognition of a misfolded protein by the molecular chaperone Hsp90. *Nat Struct Mol Biol*. 2017;24:407–413.
- Brinker A, Scheufler C, von der Mulbe F, et al. Ligand discrimination by TPR domains. Relevance and selectivity of EEVD-recognition in Hsp70 x Hop x Hsp90 complexes. *J Biol Chem*. 2002;277:19265–19275.
- Kajander T, Sachs JN, Goldman A, Regan L. Electrostatic interactions of Hsp-organizing protein tetratricopeptide domains with Hsp70 and Hsp90: Computational analysis and protein engineering. *J Biol Chem*. 2009;284:25364–25374.
- Lapelosa M. Free energy of binding and mechanism of interaction for the MEEVD-TPR2A peptide-protein complex. *J Chem Theory Comput*. 2017;13:4514–4523.
- Schopf FH, Biebl MM, Buchner J. The HSP90 chaperone machinery. *Nat Rev Mol Cell Biol*. 2017;18:345–360.
- Panaretou B, Siligardi G, Meyer P, et al. Activation of the ATPase activity of hsp90 by the stress-regulated cochaperone aha1. *Mol Cell*. 2002;10:1307–1318.
- Karagoz GE, Duarte AM, Ippel H, et al. N-terminal domain of human Hsp90 triggers binding to the cochaperone p23. *Proc Natl Acad Sci U S A*. 2011;108:580–585.
- Rohl A, Rohrberg J, Buchner J. The chaperone Hsp90: Changing partners for demanding clients. *Trends Biochem Sci*. 2013;38:253–262.
- Hallett ST, Pastok MW, Morgan RML, et al. Differential regulation of G1 CDK complexes by the Hsp90-Cdc37 chaperone system. *Cell Rep*. 2017;21:1386–1398.
- Prodromou C, Siligardi G, O’Brien R, et al. Regulation of Hsp90 ATPase activity by tetratricopeptide repeat (TPR)-domain co-chaperones. *EMBO J*. 1999;18:754–762.
- Richter K, Muschler P, Hainzl O, Reinstein J, Buchner J. Sti1 is a non-competitive inhibitor of the Hsp90 ATPase. Binding prevents the N-terminal dimerization reaction during the atpase cycle. *J Biol Chem*. 2003;278:10328–10333.
- Li J, Richter K, Buchner J. Mixed Hsp90-cochaperone complexes are important for the progression of the reaction cycle. *Nat Struct Mol Biol*. 2011;18:61–66.
- Schmid AB, Lagleder S, Grawert MA, et al. The architecture of functional modules in the Hsp90 co-chaperone Sti1/Hop. *EMBO J*. 2012;31:1506–1517.
- Scheufler C, Brinker A, Bourenkov G, et al. Structure of TPR domain-peptide complexes: Critical elements in the assembly of the Hsp70-Hsp90 multichaperone machine. *Cell*. 2000;101:199–210.
- Onuoha SC, Coulstock ET, Grossmann JG, Jackson SE. Structural studies on the co-chaperone Hop and its complexes with Hsp90. *J Mol Biol*. 2008;379:732–744.
- Southworth DR, Agard DA. Client-loading conformation of the Hsp90 molecular chaperone revealed in the cryo-EM structure of the human Hsp90:Hop complex. *Mol Cell*. 2011;42:771–781.
- Kirschke E, Goswami D, Southworth D, Griffin PR, Agard DA. Glucocorticoid receptor function regulated by coordinated action of the Hsp90 and Hsp70 chaperone cycles. *Cell*. 2014;157:1685–1697.
- Alvira S, Cuellar J, Rohl A, et al. Structural characterization of the substrate transfer mechanism in Hsp70/Hsp90 folding machinery mediated by Hop. *Nat Commun*. 2014;5:5484.

27. Oroz J, Chang BJ, Wysoczanski P, et al. Structure and pro-toxic mechanism of the human Hsp90/PPIase/Tau complex. *Nat Commun.* 2018;9:4532.
28. Tugarinov V, Kanelis V, Kay LE. Isotope labeling strategies for the study of high-molecular-weight proteins by solution NMR spectroscopy. *Nat Protoc.* 2006;1:749–754.
29. Karagoz GE, Duarte AM, Akoury E, et al. Hsp90-Tau complex reveals molecular basis for specificity in chaperone action. *Cell.* 2014;156:963–974.
30. Oroz J, Blair LJ, Zweckstetter M. Dynamic Aha1 co-chaperone binding to human Hsp90. *Protein Sci.* 2019;28:1545–1551.
31. Flom G, Behal RH, Rosen L, Cole DG, Johnson JL. Definition of the minimal fragments of Sti1 required for dimerization, interaction with Hsp70 and Hsp90 and in vivo functions. *Biochem J.* 2007;404:159–167.
32. Yi F, Doudevski I, Regan L. HOP is a monomer: Investigation of the oligomeric state of the co-chaperone HOP. *Protein Sci.* 2010;19:19–25.
33. Williamson MP. Using chemical shift perturbation to characterise ligand binding. *Prog Nucl Magn Reson Spectrosc.* 2013; 73:1–16.

### SUPPORTING INFORMATION

Additional supporting information may be found online in the Supporting Information section at the end of this article.

**How to cite this article:** Lott A, Oroz J, Zweckstetter M. Molecular basis of the interaction of Hsp90 with its co-chaperone Hop. *Protein Science.* 2020;29:2422–2432. <https://doi.org/10.1002/pro.3969>